

1 **Method Article:**

2 **An *in vitro* blood flow model to advance the study of platelet adhesion
3 utilizing a damaged endothelium**

4 Alison Leigh Banka^a and Omolola Eniola-Adefeso^{a,b*}

5 *^aDepartment of Chemical Engineering, University of Michigan, Ann Arbor, United
6 States of America; ^bDepartment of Biomedical Engineering, University of Michigan,
7 Ann Arbor, United States of America*

8 *Corresponding author. Email: lolaa@umich.edu

9

10 **Abstract**

11 *In vitro* flow assays utilizing microfluidic devices are often used to study
12 human platelets as an alternative to the costly animal models of hemostasis
13 and thrombosis that may not accurately represent human platelet behavior
14 *in vivo*. Here, we present a tunable *in vitro* model to study platelet
15 behavior in human whole blood flow that includes both an inflamed,
16 damaged endothelium and exposed extracellular matrix. We demonstrate
17 that the model is adaptable across various anticoagulants, shear rates, and
18 proteins for endothelial cell culture without the need for a complicated,
19 custom-designed device. Further, we verified the ability of this ‘damaged
20 endothelium’ model as a screening method for potential anti-platelet or
21 anti-thrombotic compounds using a P2Y₁₂ receptor antagonist (ticagrelor),
22 a pan-selectin inhibitor (Bimosiamose), and a histamine receptor
23 antagonist (Cimetidine). These compounds significantly decreased platelet
24 adhesion to the damaged endothelium, highlighting that this model can
25 successfully screen anti-platelet compounds that target platelets directly or
26 the endothelium indirectly.

27 **Keywords:** platelets; *in vitro* blood flow; endothelium; extracellular matrix
28 proteins; platelet adhesiveness

29

30 **Introduction**

31 Platelets must maintain a balancing act *in vivo* due to their contributions to both health
32 and disease. A low platelet count or underperforming platelets can disrupt hemostasis,
33 leading to bleeding risk.¹ In contrast, excess or overactive platelets can contribute to
34 thrombosis,² cardiovascular events,^{2,3} and inflammation⁴ in various diseases. The
35 adhesion of platelets to the site of vascular injury is a crucial early step in both
36 hemostasis and thrombosis, involving multiple points of binding between glycoproteins
37 (GP) on platelets and the damaged vasculature. Thus, there is great interest in
38 understanding dynamic contributions of various receptors and signal molecules that tip
39 the balance from hemostasis to thrombosis.

40 Murine models are ubiquitously employed to study hemostasis and thrombosis;
41 yet, major differences between animal and human blood physiology and disease
42 development can make translating findings from animal models to humans complicated
43 or inaccurate.⁵ Thus, many researchers turn to *in vitro* flow assays with human platelets
44 or whole blood, including the use of microfluidic devices, to study platelet adhesion and
45 behavior contributing to hemostasis and thrombosis. These *in vitro* assays typically fall
46 under one of two categories: platelets under flow conditions adhere to either patterned
47 extracellular matrix (ECM) proteins⁶ or an inflamed, intact endothelium that supports
48 platelet adhesion.^{7,8} Utilizing ECM proteins or other factors alone allows for tight
49 control of platelet adhesion to one or more specific binding motifs but neglects the
50 essential role the damaged endothelium plays in regulating thrombosis and hemostasis.⁹

51 A damaged or activated endothelium contributes to the coagulation cascade
52 through upregulation of tissue factor¹⁰ and suppression of thrombomodulin
53 expression,¹¹ among others. When the endothelium is activated, it releases Weibel-
54 Palade bodies containing ultra-long vWF,¹² which directly bind platelets from flowing

55 blood. Critically, the link between high or dysregulated vWF levels and thrombotic
56 diseases has been well-established using data from both clinical trials and animal
57 models.¹³ In addition to vWF multimers, Weibel-Palade bodies also contain P-selectin
58 that can directly bind both platelets and leukocytes upon release, recruiting them to the
59 growing thrombus.¹⁴ Moreover, a prolonged endothelial inflammation leads to
60 expression of other cell adhesion molecules, e.g., ICAM-1 and E-selectin, to further
61 recruit circulating leukocytes,¹⁵ which, when bound to the endothelium, can bind to
62 platelets to further promote thrombosis.¹⁴ Overall, the ability of the endothelium to
63 secrete vWF and other soluble factors while expressing cell adhesion molecules all
64 highlight the importance of including the endothelium in an *in vitro* model designed to
65 study platelet adhesion and resolution.

66 Indeed, endothelialized microfluidic models for studying platelet behavior have
67 gained recent attention in the literature.^{7,8} For example, researchers recently developed a
68 novel, biologically patterned 3D hydrogel that supports endothelial cell growth¹⁶ and
69 others established a 3D endothelial cell-pericyte co-culture microfluidic ‘blood vessel’
70 *in vitro*.¹⁷ While these new models represent steps towards producing more
71 physiological, 3D blood vessels *in vitro*, they have not yet been utilized to study platelet
72 behavior. Moreover, a commonality between previous endothelialized microfluidic
73 models is the reliance on a completely confluent endothelial cell monolayer, i.e., an
74 absence of a vascular injury, which does not allow for a critical first step in platelet
75 aggregation – platelet adhesion to the underlying extracellular matrix (ECM).¹⁸ One
76 recent work attempts to build in the ECM by examining platelet adhesion to a
77 deliberately non-confluent endothelium.¹⁹ Unfortunately, this approach is likely to yield
78 a wide variation in ECM spacing between endothelial cells, i.e., where platelet adhesion
79 occurs. Such lack of tight control over the ECM spacing likely limits the consistency of

80 platelet adhesion observed across experiments. Further, the endothelial cells utilized
81 were not stimulated, omitting the endothelium's role in platelet adhesion through the
82 release of vWF and expression of cell adhesion molecules.

83 Overall, there is an unmet need for an improved and tightly controlled *in vitro*
84 model that incorporates all components of a damaged vasculature *in vivo*. Here, we
85 describe a 'damaged endothelium model' that combines a functional inflamed
86 endothelium with a pronounced and consistent exposed ECM, i.e., injury area. This
87 model is straightforward, highly tunable, and allows for platelet adhesion in whole
88 blood, both to the underlying ECM and the adjacent injured endothelium, creating an
89 opportunity to elucidate the complex dynamics of platelet functions in human health
90 and disease. Further, we demonstrate that this model successfully screens potential
91 anti-inflammatory and anti-thrombotic molecules that target either platelets or the
92 endothelium.

93

94 **Methods**

95 **Materials**

96 Anti-CD41/61 PE was purchased from Biolegend (359806), and anti-vWF FITC was
97 purchased from Novus Biologicals (NB120-8822). Type I rat tail collagen was
98 purchased from Corning (354236). Adenosine diphosphate (ADP) was purchased from
99 MP Biomedicals (100056). Histamine was purchased from Acros Organics
100 (411710050). #1 ½ 30 mm round glass coverslips were purchased from Warner
101 Instruments (64-1499). The parallel plate flow chamber (PPFC) and silicone gaskets
102 were purchased from Glycotech (31-001). Cimetidine was purchased from Alfa Aesar
103 (J62825). Bimosiamose was purchased from MedChemExpress (HY-106139).
104 Ticagrelor was purchased from Cayman Chemical Company (15425). All other reagents
105 and chemicals were purchased from Sigma Aldrich or Fisher Scientific.

106 **Blood draw and preparation for flow**

107
108 Human whole blood was obtained via venipuncture and drawn into acid citrate
109 dextrose (ACD), 3.2% sodium citrate, or heparin. Informed, written consent was
110 obtained by all donors according to a protocol approved by the University of Michigan
111 Internal Review Board (IRB-MED). Unless otherwise stated, the hematocrit of the
112 anticoagulated blood was adjusted to 40% using packed RBCs or extra plasma obtained
113 from the same donor to normalize for the known impact of hematocrit on platelet
114 accumulation *in vivo* and *in vitro*.^{20,21}

115 To isolate platelets, platelet-rich plasma (PRP) was first obtained through whole
116 blood centrifugation at 200g for 20 minutes. An additional 10% ACD and 1 µL apyrase
117 per 2.5 mL PRP was added to prevent platelet activation during a 10 minute, 1000g
118 centrifugation. Isolated platelets were resuspended in a ‘flow buffer’ solution of

119 phosphate buffered saline containing calcium and magnesium ions (DPBS ^{+/+}; pH 7.4;
120 Thermo Fisher cat# 14080-055) with 1% BSA added. Packed RBCs were obtained
121 through a centrifugation of the whole blood at 2250g for 10 minutes and washed with
122 PBS – “washed RBCs”. Isolated platelets were combined with washed RBCs at a 40%
123 hematocrit for experiments utilizing platelets with RBCs in flow buffer.

124 Isolated platelets or platelets in whole blood were stained with 5 μ L/mL anti-
125 CD41/61 PE for one hour immediately prior to blood flow experiments and where
126 stated, activated with 20 μ M ADP for one hour to induce platelet activation and
127 aggregation similar to prior publications.²²⁻²⁵

128 ***Platelet adhesion to damaged monolayer under flow***

129

130 Umbilical cords (Mott Children’s Hospital, Ann Arbor) were acquired under an IRB-
131 MED approved human transfer protocol. Human umbilical vein endothelial cells
132 (HUVEC) were obtained using a modified collagenase perfusion technique,²⁶ and
133 HUVEC from three or more umbilical cords were pooled per isolation. For flow assays,
134 HUVEC were cultured at 37°C and 5% CO₂ until confluent, then trypsinized and seeded
135 onto glutaraldehyde-crosslinked gelatin coverslips at least 36 hours before use.
136 Glutaraldehyde-crosslinked gelatin coverslips were achieved via coating glass
137 coverslips with 1% w/v gelatin crosslinked with 0.5% glutaraldehyde, which was
138 quenched with 0.1 M glycine and washed with PBS.²⁷

139 In flow experiments utilizing an endothelium, HUVEC were activated for 2
140 minutes with 100 μ M histamine in media. After 2 minutes, a scalpel was used to scratch
141 the coverslip with parallel lines to induce an acute vascular injury and expose the
142 underlying gelatin. The coverslip was attached to a PPFC fitted with a silicone gasket (2
143 cm x 0.25 cm x 127 μ m in height) via vacuum pump and the outlet was attached to a

144 syringe pump. The blood or blood components were perfused over the damaged
145 HUVEC perpendicular to the scalpel scores for 5 minutes at a fixed wall shear rate
146 described by Equation 1:

147

$$\gamma_w = \frac{6Q}{h^2 w} \quad (1)$$

148 Where Q is the volumetric flow rate (mL/s), h is the channel height (0.0127 cm),
149 and w is the channel width (0.25 cm). After 5 minutes of laminar flow, the channel was
150 rinsed with flow buffer and 10 fluorescent images of platelets bound along the scalpel
151 scores were taken.

152 In experiments testing different agonists to induce vWF secretion, HUVEC on
153 coverslips were activated by calcium ionophore (10 μ M) for 10 minutes, or histamine
154 (100 μ M) for 2 minutes with or without mechanical injury with a scalpel before being
155 attached to a PPFC. To visualize vWF multimer strands, 5 μ g/mL anti-vWF-FITC was
156 flowed over the endothelium for 5 minutes and rinsed with flow buffer for 5 minutes. 10
157 fluorescent images of vWF multimers around the scalpel scores were taken.

158 Where stated, whole blood was treated with 50 μ M Bimosiamose or with 10 μ M
159 ticagrelor in other experiments for 1 hour prior to use in flow experiments. In other
160 experiments, HUVEC were pretreated with 1 or 50 μ M Cimetidine for 5 hours prior to
161 use in flow experiments.

162 ***Platelet adhesion to collagen and gelatin-coated coverslips under flow***

163 Glass coverslips were cleaned with Piranha solution (3:1 concentrated sulfuric acid:
164 30% hydrogen peroxide) and silanated with 2% 3-(trimethoxysilyl)propyl methacrylate
165 (MPS) by volume in 95% ethanol for 30 minutes. The cleaned coverslips were coated
166 with 1 mg/mL collagen or gelatin for 2 hours at room temperature; the entire coverslip

167 surface was coated with collagen or gelatin. After the 2-hour incubation, the coverslips
168 were rinsed with PBS, then attached to the PFFC and perfused with blood as described
169 above.

170 ***Statistics***

171 Ten fluorescent images of adherent platelets were acquired for each experiment, with n
172 ≥ 3 for each data point presented. ImageJ was utilized to determine the % area of the
173 'damaged endothelium' covered by platelets, which combined adhesion to the intact
174 endothelium and the exposed extracellular matrix. In short, the background fluorescence
175 for each image was subtracted and threshold set. ImageJ then calculated the surface area
176 coverage of each image using the threshold. Data are plotted with standard error bars.
177 Student's unpaired t-tests and one- and two-way ANOVA in GraphPad Prism software
178 were used to analyze statistical differences between samples. Asterisks indicate p values
179 of $* < 0.05$, $** < 0.01$, $*** < 0.001$, and $**** < 0.0001$. A lack of asterisks indicates a
180 lack of significance.

181

182 **Results and Discussion**

183 ***Development of an in vitro flow model utilizing an endothelium***

184 Our first goal in developing an *in vitro* model to better represent platelet adhesion *in*
185 *vivo* was to determine the agonists that would result in a consistent release of vWF
186 multimers from a damaged endothelium. We subjected a monolayer of human umbilical
187 vein endothelial cells (HUVECs) to either a scalpel score mechanical injury, chemical
188 stimulation (histamine or calcium ionophore), or a combination of mechanical injury
189 and chemical stimulation. Chemical stimulation via histamine alone increases vWF
190 secretion by HUVEC (Fig. 1A), which is further enhanced with the addition of a
191 mechanical injury. Mechanical injury induces platelet adhesion in two separate ways; it
192 increases vWF secretion by HUVEC, a primary first step in hemostasis (Fig. 1A), while
193 also exposing the underlying ECM proteins. Manual damage via scalpel scores resulted
194 in a ‘gap’ in the confluent HUVEC monolayer of approximately $157 \pm 3 \mu\text{m}$; a
195 representative brightfield image of the damaged HUVEC, with an EC-free gap visible,
196 overlaid with fluorescent imaging of fluorescently-labeled platelets is shown in
197 Supplementary Figure 1. Figure 1B demonstrates that the ‘damaged endothelium’
198 model facilitates the adhesion of ADP-activated human platelets to both tethered vWF
199 multimers and the underlying ECM proteins. Overall, the injury condition in which both
200 histamine stimulation and mechanical injury are present resulted in the largest increase
201 in vWF secretion compared to the other conditions (Fig. 1A) and so was utilized for all
202 other assays.

203 Previous works examining whole blood platelet adhesion in fluidic devices
204 observed differing platelet adhesion behavior across varying shear rates. These
205 discrepancies may be due to studies utilizing different flow channels, microfluidic
206 surface coatings for platelet adhesion, and anticoagulants. As such, we examined the

207 impact of shear on platelet adhesion after establishing the damaged endothelium flow
208 model. Blood flow is represented here using shear rates as opposed to volumetric flow
209 rates due to the latter's known direct impact on convective transport of soluble factors
210 as well as cell-surface interactions.²⁸ We chose a range of shear rates representative of
211 blood flow in different vessels *in vivo*. Specifically, we utilized 100s⁻¹ (representing
212 blood flow in veins), 500s⁻¹ (representing large arteries), and 1000s⁻¹ (representing
213 arterioles and capillaries).⁷ Activation of platelets in whole blood with 20 μ M ADP led
214 to increased platelet adhesion across all shear rates tested (100, 500, and 1000s⁻¹; Fig.
215 1C) in comparison to flow experiments utilizing resting platelets. This increase in
216 adhesion highlights the known ability of ADP to stimulate platelets, an essential step in
217 platelet adhesion at shear rates <1000s⁻¹.²⁹ Further, activated platelet adhesion at low
218 shear rates (100s⁻¹) was higher than that at higher shear rates (500 and 1000s⁻¹). This
219 observation aligns with other works that observed maximal platelet adhesion at low
220 shear rates in whole blood – an impact the authors hypothesized was due to the lag time
221 in plasma protein adsorption onto the microfluidic surface at high shear rates.³⁰

222 To further explore the binding mechanism and the role of different components
223 of blood in this model, we examined activated platelet adhesion in buffer alone or buffer
224 containing human RBCs at 40% hematocrit. Platelet adhesion in buffer flow was
225 greatest at high shear rates (1000s⁻¹; Fig. 1D). In the absence of plasma, high shear
226 allows for ultra-long vWF multimers released from activated endothelial cells to
227 elongate and expose adhesion sites without cleavage by plasma ADAMTS-13,
228 enhancing platelet binding.^{31,32} Previous works determined that HUVEC in flow do not
229 release sufficient quantities of ADAMTS-13 to cleave ultra-long vWF multimers
230 tethered to their surface without the presence of healthy plasma or purified ADAMTS-
231 13.^{12,31,33} Therefore, the high level of platelet adhesion in buffer at high shear rates

232 suggests that vWF plays an important role in this model. As expected, the addition of
233 RBCs to platelets in buffer increased platelet flow adhesion at all shear rates (Fig. 1D),
234 highlighting the importance of RBCs to facilitate margination of platelets towards the
235 vascular wall and increasing binding to the damaged endothelium.³⁴ Representative
236 images of activated platelet adhesion at 1000s⁻¹ in whole blood, isolated in buffer, and
237 isolated in buffer with the addition of RBCs are shown in Fig. 1E. For all conditions,
238 platelet adhesion predominates at and around the scalpel score and adjacent
239 endothelium area, i.e., the injury region, including adhesion to long vWF strings
240 attached to the endothelium at high shear rates.

241 We confirmed that our model supports platelet adhesion across various
242 anticoagulants as reported in Supplementary Figure 2A for adhesion at 1000s⁻¹ of
243 platelets in blood anticoagulated with ACD, heparin, and sodium citrate. We find the
244 highest platelet adhesion occurred when sodium citrate (3.2%) is used as the
245 anticoagulant, leading to a significant increase in platelet coverage compared to ACD-
246 anticoagulated blood. Adherent platelets are primarily localized to the area with and
247 near the scalpel score for all anticoagulant types, as illustrated in Supplementary Figure
248 2B. Importantly, the presence of the endothelium in our model does not preclude its
249 utility for testing anti-platelet compounds in blood flow. Specifically, we find that
250 addition of ticagrelor, a P2Y₁₂ receptor binding antagonist, to blood led to a significant
251 decrease in activated platelet adhesion relative to adhesion in untreated blood, which
252 was consistent across both ACD and heparin anticoagulated whole blood
253 (Supplementary Figure 3).

254 ***Platelet adhesion on damaged endothelium is similar to controls utilizing***
255 ***collagen and gelatin***
256 A common method of examining platelet behavior in flow involves platelet adhesion to

257 patterned ECM proteins, especially collagen. To determine how platelet adhesion using
258 our 'damaged endothelium' model compared to the standard, we examined platelet
259 adhesion in whole blood flow to the damaged endothelium and collagen alone at 1
260 mg/mL.^{30,35,36} We included another control of platelet adhesion to gelatin alone at the
261 same concentration as collagen because crosslinked gelatin is used in our damaged
262 endothelium model. Fig. 2 shows that when platelets in blood are activated, they adhere
263 with the same frequency to the damaged HUVEC model as collagen alone; there was no
264 difference between the magnitude of platelet adhesion to the damaged HUVEC model
265 and collagen at any of the shear rates examined. Qualitatively, platelet adhesion to
266 collagen was distributed randomly in small aggregates on the collagen surface.
267 Conversely, platelet adhesion to the damaged endothelium was primarily concentrated
268 on the exposed ECM between endothelial cells for all shear rates examined and on the
269 long, vWF strands bound to the endothelium for higher shear rates examined. Adhesion
270 to collagen alone follows the same trend of higher adhesion under low shear rate
271 conditions (100s^{-1}) than higher shear conditions ($500, 1000\text{s}^{-1}$). Platelet adhesion to
272 gelatin followed similar trends, but adhesion at 100s^{-1} was significantly lower than
273 platelet adhesion to collagen at the same shear rate, suggesting that gelatin alone at 1
274 mg/mL does not facilitate platelet adhesion as well as collagen. Conversely, when
275 platelets were resting, there were no significant differences between adhesion to the
276 damaged HUVEC, collagen, or gelatin at any of the shear rates tested (Supplementary
277 Figure 4).

278 ***Treatment of whole blood with pan-selectin inhibitor decreases platelet
279 adhesion to damaged endothelium***

280 One benefit of utilizing the damaged endothelium model is the inclusion of multiple
281 binding motifs for platelets, both the damaged endothelium itself and the underlying

282 extracellular matrix proteins. These multiple binding motifs make this model ideal for
283 screening potential drug compounds that impact platelet adhesion in human whole
284 blood flow. One compound of interest is Bimosiamose, a siayl Lewis^x mimetic and pan-
285 selectin inhibitor.³⁷ Despite the ability of this antagonistic compound to target E-
286 selectin, P-selectin, and L-selectin, Bimosiamose has primarily been studied for its
287 ability to inhibit leukocyte binding and recruitment *in vitro*,³⁷ *in vivo*,^{38,39} and in clinical
288 trials.^{40,41}

289 To determine if Bimosiamose's ability to inhibit selectins could impact platelet
290 adhesion in the damaged endothelium model, we pretreated whole blood with 50 μ M
291 Bimosiamose for 1 hour prior to flow experiments. Like all previous experiments, we
292 stimulated the endothelium with histamine with mechanical injury via scalpel, which
293 does not facilitate the adhesion of leukocytes in blood flow; these conditions allow us to
294 examine the impact of Bimosiamose on platelet adhesion alone. We treated blood with
295 ADP to induce platelet activation at the same time as Bimosiamose. The Bimosiamose
296 treatment led to a 40% reduction in activated platelet adhesion to the damaged
297 endothelium model relative to its untreated counterparts (Fig. 3). In comparison, whole
298 blood pretreated with Bimosiamose and flowed over collagen only coverslips did not
299 impact platelet adhesion (Fig. 3). We attribute Bimosiamose's effectiveness in
300 decreasing platelet adhesion on the damaged endothelium to the increased platelet
301 binding motifs present that are not present on the collagen substrate. Specifically, we
302 hypothesize that Bimosiamose in whole blood blocked the GPIb-IX-V receptor complex
303 on platelets that binds to P-selectin on the endothelium.¹⁸ The lack of P-selectin on
304 collagen alone renders this blocking impact inconsequential. Further, excess
305 Bimosiamose in blood may also have blocked P-selectin on the endothelial cell surface
306 once blood flow through the chamber began. The capability of Bimosiamose to block

307 leukocyte adhesion via blocking of selectins has been well established.³⁷⁻⁴¹ However,
308 we demonstrated that Bimosiamose further has the ability to directly modulate platelet
309 behavior in the complete absence of leukocyte adhesion.

310 To confirm that the impact Bimosiamose has on ACD-anticoagulated platelets is
311 translatable to other anticoagulants, we examined the impact of Bimosiamose on
312 activated platelet adhesion in heparinized blood. Bimosiamose led to a significant
313 decrease in platelet adhesion to the damaged endothelium using heparin as an
314 anticoagulant (Supplementary Figure 5); further, there was no significant difference
315 between the change in ACD-anticoagulated platelet adhesion and heparin-
316 anticoagulated platelet adhesion when treated with Bimosiamose. We are thus able to
317 confirm that results obtained using ACD-anticoagulated blood translate to other
318 commonly used anticoagulants.

319 ***Treatment of damaged endothelium with Cimetidine decreases platelet adhesion***

320 The inclusion of the endothelium in this model also allows for the testing of compounds
321 that have a direct therapeutic impact on the endothelium instead of on platelets
322 themselves. One potential candidate to screen for impact on platelet adhesion is
323 Cimetidine, a histamine receptor antagonist marketed under the brand name ‘Tagamet’
324 to treat heartburn and peptic ulcers. More recently, Cimetidine has gained interest for its
325 ability to inhibit the expression of selectins by endothelial cells. In particular,
326 Cimetidine was found to decrease neutrophil adhesion to endothelial cells activated by
327 high concentrations of glucose, decreasing the expression of cellular adhesion
328 molecules P-selectin and ICAM-1 on the surface of HUVEC.⁴² Further, Cimetidine has
329 been repurposed in combination with other oncological therapeutics and
330 pharmaceuticals in a variety of clinical trials for different cancers to capitalize on

331 several qualities of Cimetidine, including its ability to inhibit cancer cell adhesion to
332 endothelial cells.⁴³

333 To take advantage of Cimetidine's ability to decrease cellular adhesion molecule
334 expression as well as its histamine receptor antagonism, we treated HUVEC with low (1
335 μ M) or high (50 μ M) concentrations of Cimetidine 5 hours prior to use in blood flow
336 experiments. Similar to all previous experiments, we treated the endothelium only with
337 histamine and mechanical injury to determine if Cimetidine has an effect on platelet
338 adhesion in the absence of adherent leukocytes. Due to treating the endothelium itself
339 with Cimetidine instead of whole blood, there was no corresponding collagen-only
340 control for this experiment. Treatment with either low or high concentrations of
341 Cimetidine significantly decreased activated platelet adhesion to approximately 67% of
342 untreated HUVEC, demonstrating that even a low dosage of the compound was enough
343 to significantly decrease platelet adhesion in this model. This knockdown in platelet
344 adhesion occurred even in the absence of leukocyte adhesion, highlighting Cimetidine's
345 effectiveness at modulating platelet adhesion behavior. Further, this experiment
346 demonstrates that this damaged endothelium model can be used to screen potential
347 therapeutics for impact on platelet adhesion, even if the target of the therapeutic is the
348 endothelium instead of platelets themselves.

349 **Conclusions**

350 *In vitro* microfluidic models are an excellent way to study human platelet behavior in a
351 laboratory setting to better understand hemostasis and thrombosis. However, most
352 models utilize simple protein substrates patterned onto glass or plastic to study platelet
353 behavior, which neglects the role of the endothelium in clotting and clot resolution.
354 Alternatively, other models utilize confluent endothelial monolayers that neglect

355 platelet adhesion to exposed extracellular matrix proteins. Here, we described a novel,
356 *in vitro* flow model utilizing a damaged endothelium that allows for the study of platelet
357 binding to both the endothelium and underlying extracellular matrix proteins without
358 requiring the design and production of custom microfluidic devices. Further, the model
359 is tunable depending on the specific needs of the user. Platelet adhesion to the damaged
360 endothelium occurs at various shear rates and across different anticoagulants. As a proof
361 of concept, two potential therapeutics were screened for their ability to impact platelet
362 adhesion; the pan-selectin inhibitor Bimosiamose significantly decreased activated
363 platelet adhesion to the damaged endothelium, as did Cimetidine. The screening of
364 these two compounds demonstrates the ability of this damaged endothelium model as an
365 initial screening method of potential anti-thrombotic or anti-platelet compounds that can
366 impact either platelets or the endothelium itself and represents a novel method to study
367 future platelet-cell and platelet-drug interactions.

368 A limitation of this work is that only one specific type of protein was utilized for
369 HUVEC culture (gelatin). However, since glutaraldehyde crosslinks proteins by
370 reacting with their free primary amines⁴⁴, proteins of interest other than gelatin can be
371 utilized for HUVEC culture with this method. Future work utilizing this adaptive
372 model can explore how tuning the crosslinked protein or proteins can alter platelet
373 behavior, in addition to elucidating the behavior of endothelial cells isolated from
374 different vascular beds with shear rates corresponding to those vessels (i.e., studying
375 saphenous vein endothelial cells at $\sim 100\text{s}^{-1}$ in contrast to coronary artery endothelial
376 cells at $\sim 400\text{s}^{-1}$,⁷).

377
378

379 **Availability of Data:**

380 All data generated or analyzed during this study are included in this published article and
381 supplementary material. The raw datasets in this current study are available from the
382 corresponding author on reasonable request. Identity of study participants will not be
383 shared.

384

385 **Competing Interests:**

386 The authors declare no competing interests.

387

388 **Funding:** This work was in part supported by an NSF Research Grant (CBET1854726)
389 and Falk Medical Research Trust Catalyst Award to O.E.A. A.L.B was supported by
390 NIH Cellular Biotechnology Training Grant.

391 **Author Contributions:** A.L.B and O.E-A. conceived and designed the experimental
392 protocols. A.L.B. prepared all blood samples for measurement and analyzed all the
393 collected data. A.L.B. and O. E-A. wrote the manuscript. All authors read and approved
394 the final manuscript.

395

396 **References**

397 1. Piel-Julian M, Mahevas M, Germain J, Languille L, Comont T, Lapeyre-Mestre
398 M, Payrastre B, Beyne-Rauzy O, Godeau B, Adoue D, *et al.* Risk factors for
399 bleeding, including platelet count threshold, in newly diagnosed immune
400 thrombocytopenia adults. *J Thromb Haemost*. 2018; 16(9): 1830–1842. doi:
401 10.1111/jth.14227.

402 2. Patti G, Di Martino G, Ricci F, Renda G, Gallina S, Hamrefors V, Melander O,
403 Sutton R, Engström G, De Caterina R, *et al.* Platelet Indices and Risk of Death
404 and Cardiovascular Events: Results from a Large Population-Based Cohort
405 Study. *Thromb Haemost*. 2019; 119 (11): 1773-1784. doi: 10.1055/s-0039-
406 1694969

407 3. Christie DJ, Kottke-Marchant K, Gorman RT. Hypersensitivity of platelets to
408 adenosine diphosphate in patients with stable cardiovascular disease predicts
409 major adverse events despite antiplatelet therapy. *Platelets*. 2008; 19 (2): 104–
410 110. doi: 10.1080/09537100701504095

411 4. Davila J, Manwani D, Vasovic L, Avanzi M, Uehlinger J, Ireland K, Mitchell
412 WB. A novel inflammatory role for platelets in sickle cell disease. *Platelets*.
413 2015; 26 (8): 726–729. doi: 10.3109/09537104.2014.983891

414 5. Cooley BC. Murine models of thrombosis. *Thromb Res*. 2012; 129: S62-S64.
415 doi: 10.1016/j.thromres.2012.02.036.

416 6. Schoeman RM, Lehmann M, Neeves KB. Flow chamber and microfluidic
417 approaches for measuring thrombus formation in genetic bleeding disorders.
418 *Platelets*. 2017; 28 (5): 463–471. doi: 10.1080/09537104.2017.1306042.

419 7. Coenen DM, Mastenbroek TG, Cosemans, J. Platelet interaction with activated
420 endothelium: Mechanistic insights from microfluidics. *Blood*. 2017; 130 (26)
421 2819–2828. doi: 10.1182/blood-2017-04-780825.

422 8. Zilberman-Rudenko J, Sylman JL, Garland KS, Puy C, Wong AD, Searson PC,
423 McCarty O. Utility of microfluidic devices to study the platelet–endothelium
424 interface. *Platelets*. 2017; 28 (5) 449–456. doi:
425 10.1080/09537104.2017.1280600.

426 9. Yau JW, Teoh H, Verma S. Endothelial cell control of thrombosis. *BMC*
427 *Cardiovasc Disord*. 2015; 15 (130). doi: 10.1186/s12872-015-0124-z.

428 10. Reiner MF, Akhmedov A, Stivala S, Keller S, Gaul DS, Bonetti NR, Savarese
429 G, Glanzmann M, Zhu C, Ruf W, *et al.* Ticagrelor, but not clopidogrel, reduces
430 arterial thrombosis via endothelial tissue factor suppression. *Cardiovasc Res.*
431 2017; 113 (1): 61–69. doi: 10.1093/cvr/cvw233.

432 11. Lin PY, Shen HC, Chen CJ, Wu SE, Kao HL, Huang JH, Wang DL, Chen SC.
433 The inhibition in tumor necrosis factor- α -induced attenuation in endothelial
434 thrombomodulin expression by carvedilol is mediated by nuclear factor- κ B and
435 reactive oxygen species. *J Thromb Thrombolysis.* 2010; 29 (1): 52–59. doi:
436 10.1007/s11239-009-0318-2.

437 12. Turner NA, Nolasco L, Ruggeri ZM, Moake, JL. Endothelial cell ADAMTS-13
438 and VWF: production, release, and VWF string cleavage. *Blood.* 2009; 114 (24):
439 5102–5111. doi: 10.1182/blood-2009-07-231597.

440 13. Xiang Y, Hwa J. Regulation of VWF expression, and secretion in health and
441 disease. *Curr Opin Hematol.* 2016; 23 (3): 288–293. doi:
442 10.1097/MOH.0000000000000230.

443 14. Li J, Kim K, Barazia A, Tseng A, Cho J. Platelet-neutrophil interactions under
444 thromboinflammatory conditions. *Cell Mol Life Sci.* 2015; 72 (14): 2627–2643.
445 doi: 10.1007/s00018-015-1845-y.

446 15. Haraldsen G, Kvale D, Lien B, Farstad IN, Brandtzaeg P. Cytokine-Regulated
447 Expression of E-Selectin, Intercellular Adhesion Molecule-1 (ICAM-1), and
448 Vascular Cell Adhesion Molecule-1 (VCAM-1) in Human Intestinal
449 Microvascular Endothelial Cells. *J Immunol.* 1996; 156 (7): 2558–2565. PMID:
450 8786319.

451 16. Loessberg-Zahl J, Beumer J, van den Berg A, Eijkel JCT, van der Meer AD.
452 Patterning Biological Gels for 3D Cell Culture inside Microfluidic Devices by
453 Local Surface Modification through Laminar Flow Patterning. *Micromachines.*
454 2020; 11 (12): 1112. doi: 10.3390/MI11121112.

455 17. van Dijk CGM, Brandt MM, Poulis N, Anten J, van der Moolen M, Kramer L,
456 Homburg EFGA, Louzao-Martinez L, Pei J, Krebber MM, *et al.* A new
457 microfluidic model that allows monitoring of complex vascular structures and
458 cell interactions in a 3D biological matrix. *Lab Chip* 2020; 20 (10) 1827–1844.
459 doi: 10.1039/D0LC00059K.

460 18. Ruggeri ZM, Mendolicchio GL. Adhesion mechanisms in platelet function. *Circ Res.* 2007; 100 (12): 1673–1685. doi: 10.1161/01.RES.0000267878.97021.ab.

461 19. Brouns SLN, Provenzale I, van Geffen JP, van der Meijden PEJ, Heemskerk JWM. Localized endothelial-based control of platelet aggregation and coagulation under flow: A proof-of-principle vessel-on-a-chip study. *J. Thromb. Haemost.* 2020; 18 (4) 931–941. doi: 10.1111/JTH.14719.

462 20. Walton BL, Lehmann M, Skorczewski T, Holle LA, Beckman JD, Cribb JA, Mooberry MJ, Wufsus AR, Cooley BC, Homeister JW, *et al.* Elevated hematocrit enhances platelet accumulation following vascular injury. *Blood.* 2017; 129 (18) 2537–2546. doi: 10.1182/blood-2016-10-746479.

463 21. Chen H, Angerer JI, Napoleone M, Reininger AJ, Schneider SW, Wixforth A, Schneider MF, Alexander-Katz A. Hematocrit and flow rate regulate the adhesion of platelets to von Willebrand factor. *Biomicrofluidics.* 2013; 7 (6) 64113. doi: 10.1063/1.4833975.

464 22. Sibbing D, Braun S, Jawanski S, Vogt W, Mehilli J, Schömig A, Kastrati A, von Beckerath N. Assessment of ADP-induced platelet aggregation with light transmission aggregometry and multiple electrode platelet aggregometry before and after clopidogrel treatment. *Thromb. Haemost.* 2008; 99 (1) 121-126. doi: 10.1160/TH07-07-0478.

465 23. Gurbel PA, Bliden KP, Etherington A, Tantry US. Assessments of clopidogrel responsiveness: Measurements of maximum platelet aggregation, final platelet aggregation and their correlation with vasodilator-stimulated phosphoprotein in resistant patients. *Thromb. Res.* 2007; 121 (1) 107-115. doi: 10.1016/J.THRMRES.2007.02.007.

466 24. Lecka, J. Rana MS, Sevigny J. Inhibition of vascular ectonucleotidase activities by the pro-drugs ticlopidine and clopidogrel favours platelet aggregation. *Br. J. Pharmacol.* 2010; 161 (5) 1150-1160. doi: 10.1111/J.1476-5381.2010.00951.X.

467 25. Lu Y, Li Q, Liu YY, Sun K, Fan JY, Wang CS, Han JY. Inhibitory effect of caffeic acid on ADP-induced thrombus formation and platelet activation involves mitogen-activated protein kinases. *Sci. Rep.* 2015; 5 (1) 1-13. doi: 10.1038/srep13824.

468 26. Huang AJ, Furie MB, Nicholson SC, Fischbarg J, Liebovitch LS, Silverstein SC. Effects of human neutrophil chemotaxis across human endothelial cell

493 monolayers on the permeability of these monolayers to ions and
494 macromolecules. *J. Cell. Physiol.* 1988; 135 (3) 355–366. doi:
495 10.1002/JCP.1041350302.

496 27. Huang RB, Eniola-Adefeso O. Shear Stress Modulation of IL-1 β -Induced E-
497 Selectin Expression in Human Endothelial Cells. *PLoS One.* 2012; 7 (2) e31874.
498 doi: 10.1371/journal.pone.0031874.

499 28. Panteleev MA, Korin N, Reesink KD, Bark DL, Cosemans JM, Gardiner EE,
500 Mangin PH. Wall shear rates in human and mouse arteries: Standardization of
501 hemodynamics for in vitro blood flow assays: Communication from the ISTH
502 SSC subcommittee on biorheology. *J. Thromb. Haemost.* 2021; 19 (2) 588–595.
503 doi: 10.1111/jth.15174.

504 29. Jackson SP, Nesbitt WS, Westein, E. Dynamics of platelet thrombus formation.
505 *J Thromb Haemost.* 2009; 7 (s1): 17–20. doi: 10.1111/j.1538-
506 7836.2009.03401.x.

507 30. Neeves KB, Onasoga AA, Hansen RR, Lilly JJ, Venckunaite D, Sumner MB,
508 Irish AT, Brodsky G, Manco-Johnson MJ, DiPaola JA. Sources of Variability in
509 Platelet Accumulation on Type 1 Fibrillar Collagen in Microfluidic Flow
510 Assays. *PLoS One.* 2013; 8 (1): e54680. doi: 10.1371/journal.pone.0054680.

511 31. Dong J, Moake JL, Nolasco L, Bernardo A, Arceneaux W, Shrimpton CN,
512 Schade AJ, McIntire LV, Fujikawa K, Lopez JA. ADAMTS-13 rapidly cleaves
513 newly secreted ultralarge von Willebrand factor multimers on the endothelial
514 surface under flowing conditions. *Blood.* 2002; 100 (12): 4033–4039. doi:
515 10.1182/blood-2002-05-1401.

516 32. Huizinga EG, Tsuji S, Romijn RAP, Schiphorst ME, de Groot PG, Sixma JJ,
517 Gros P. Structures of glycoprotein Ib α and its complex with von Willebrand
518 factor A1 domain. *Science.* 2002; 297 (5584): 1176–1179. doi:
519 10.1126/science.107355.

520 33. Turner N, Nolasco L, Dong JF, Moake J. ADAMTS-13 cleaves long von
521 Willebrand factor multimeric strings anchored to endothelial cells in the absence
522 of flow, platelets or conformation-altering chemicals. *J Thromb Haemost.* 2009;
523 7 (1): 229–232. doi: 10.1111/j.1538-7836.2008.03209.x.

524 34. Kim S, Kai Ong P, Yalcin O, Intaglietta M, Johnson, PC. The cell-free layer in
525 microvascular blood flow. *Biorheology*. 2009; 46 (3): 181–189. doi:
526 10.3233/BIR-2009-0530.

527 35. Bark DL, Para AN, Ku DN. Correlation of thrombosis growth rate to
528 pathological wall shear rate during platelet accumulation. *Biotechnol Bioeng*.
529 2012; 109 (10): 2642–2650. doi: 10.1002/bit.24537.

530 36. Chen Z, Zhang J, Kareem K, Tran D, Conway RG, Arias K, Griffith BP, Wu ZJ.
531 Device-induced platelet dysfunction in mechanically assisted circulation
532 increases the risks of thrombosis and bleeding. *Artif. Organs*. 2019; 43 (8): 745–
533 755. doi: 10.1111/aor.13445.

534 37. Kogan TP, Dupré B, Bui H, McAbee KL, Kassir JM, Scott IL, Hu X,
535 Vanderslice P, Beck PJ, Dixon RAF. Novel synthetic inhibitors of selectin-
536 mediated cell adhesion: Synthesis of 1,6-bis[3-(3-carboxymethylphenyl)-4-(2- α -
537 D-mannopyranosyloxy)phenyl] hexane (TBC1269). *J Med Chem*. 1998; 41 (7):
538 1099–1111. doi: 10.1021/jm9704917.

539 38. Hicks AER, Abbott KB, Dodd P, Ridger VC, Hellewell PG, Norman KE. The
540 anti-inflammatory effects of a selectin ligand mimetic, TBC-1269, are not a
541 result of competitive inhibition of leukocyte rolling in vivo. *J Leukoc Biol*.
542 2005; 77 (1) 59–66. doi: 10.1189/jlb.1103573.

543 39. Ramos-Kelly JR, Toledo-Pereyra LH, Jordan J, Rivera-Chavez F, Rohs T,
544 Holevar M, Dixon RAF, Yun E, Ward PA. Multiple Selectin Blockade with a
545 Small Molecule Inhibitor Downregulates Liver Chemokine Expression and
546 Neutrophil Infiltration after Hemorrhagic Shock. *J Trauma Inj Infect Crit Care*.
547 2000; 49 (1) 92–100. doi: 10.1097/00005373-200007000-00015.

548 40. Watz H, Bock D, Meyer M, Schierhorn K, Vollhardt K, Woischwill C, Pedersen
549 F, Kirsten A, Beeh KM, Meyer-Sabellek W, *et al.* Inhaled pan-selectin
550 antagonist Bimosiamose attenuates airway inflammation in COPD. *Pulm
551 Pharmacol Ther*. 2013; 26 (2) 265–270. doi: 10.1016/j.pupt.2012.12.003.

552 41. Kirsten A, Watz H, Kretschmar G, Pedersen F, Bock D, Meyer-Sabellek W,
553 Magnussen H. Efficacy of the pan-selectin antagonist Bimosiamose on ozone-
554 induced airway inflammation in healthy subjects - A double blind, randomized,
555 placebo-controlled, cross-over clinical trial. *Pulm Pharmacol Ther*. 2011; 24 (5)
556 555–558. doi: 10.1016/j.pupt.2011.04.029.

557 42. Takeuchi Y, Okayama N, Imaeda K, Okouchi M, Omi H, Imai S, Akao M,
558 Takeda Y, Hukutomi T, Itoh M. Effects of histamine 2 receptor antagonists on
559 endothelial-neutrophil adhesion and surface expression of endothelial adhesion
560 molecules induced by high glucose levels. *J Diabetes Complications*. 2007; 21
561 (1) 50–55. doi: 10.1016/j.jdiacomp.2006.02.002.

562 43. Pantziarka P, Bouche G, Meheus L, Sukhatme V, Sukhatme VP. Repurposing
563 drugs in oncology (ReDo)-cimetidine as an anti-cancer agent.
564 *Ecancermedicalscience*. 2014; 8: 485. doi: 10.3332/ecancer.2014.485.

565 44. Kawahara J, Ishikawa K, Uchimaru T, Takaya H. Chemical Cross-Linking by
566 Glutaraldehyde between Amino Groups: Its Mechanism and Effects. In: Swift
567 G, Carraher CE, Bowman CN, editors. *Polymer Modification*. Boston (MA):
568 Springer; 1997. p. 119–131. doi:10.1007/978-1-4899-1477-4_11.

569 **Figure Legend**

570 Figure 1: Development of in vitro flow model utilizing an endothelium. (A) Change in
571 median fluorescent intensity (MFI) of von Willebrand factor secreted by cultured
572 HUVEC in comparison to unstimulated controls, (B) Representative fluorescence image
573 of endothelium activated with histamine and physically disrupted with scalpel (scalpel
574 mark shown in white), allowing for adhesion of activated, isolated platelets in buffer
575 flow containing RBCs. Green represents von Willebrand factor multimers (labelled with
576 anti-vWF FITC) and red represents adherent platelets (labelled with anti-CD41/61 PE),
577 scale bar 200 μ m., (C) Platelet coverage (as % of total surface area of photo) after 5
578 minutes of laminar flow in whole blood at a 40% hematocrit and 1000s⁻¹ on histamine-
579 stimulated and mechanically disrupted HUVEC. Platelets were either quiet or activated
580 with 20 μ M ADP, (D). Platelet coverage (%) on damaged endothelium of activated
581 platelets after 5 minutes of laminar flow. Activated platelets were anticoagulated with
582 ACD at varying shear rates either in whole blood at 40% hematocrit, isolated in flow
583 buffer, or in flow buffer with RBCs at 40% hematocrit, (E) Representative image of
584 adherent, activated platelets (red) on damaged endothelium after 5 minutes of laminar
585 flow at 1000s⁻¹ in whole blood at 40% hematocrit, isolated platelets in flow buffer, or
586 isolated platelets and RBCs at 40% hematocrit in flow buffer, scale bar 100 μ m.
587 Statistical analyses were performed using one-way ANOVA (A) or two-way ANOVA
588 (C, D) with Tukey's multiple comparisons test, where (*) indicates p<0.05, (**)
589 indicates p<0.01, (***) indicates p<0.001, and (****) indicates p<0.0001.

590 Figure 2: Platelet adhesion on damaged endothelium in comparison to controls ECM
591 proteins. Platelet coverage (as % of total surface area of photo) on damaged
592 endothelium, collagen (1 mg/mL), or gelatin (1 mg/mL) of activated platelets in whole
593 blood at 40% hematocrit after 5 minutes of laminar flow. Statistical analyses were
594 performed using two-way ANOVA with Tukey's multiple comparisons test, where (*)
595 indicates p<0.05.

596 Figure 3: Pan-selectin inhibitor decreases platelet adhesion to HUVEC. Activated
597 platelet adhesion fold change on damaged HUVEC or collagen alone of whole blood at
598 40% hematocrit at 1000s⁻¹ for 5 minutes with the addition of 50 μ M Bimosiamose to
599 whole blood 1 hour before flow experiments. Statistical analyses were performed using
600 Student's unpaired t-test where (****) indicates p<0.001.

601 Figure 4: Platelet adhesion to damaged HUVEC decreases with Cimetidine pretreatment
602 of HUVEC. Activated platelet adhesion fold change on damaged HUVEC of whole
603 blood at 40% hematocrit at 1000s^{-1} for 5 minutes with the addition of 1 μM (low) or 50
604 μM (high) Cimetidine to HUVEC 5 hours prior to blood flow experiments. Statistical
605 analyses were performed using one-way ANOVA with Dunnett's multiple comparisons
606 test where (*) indicates $p < 0.05$.

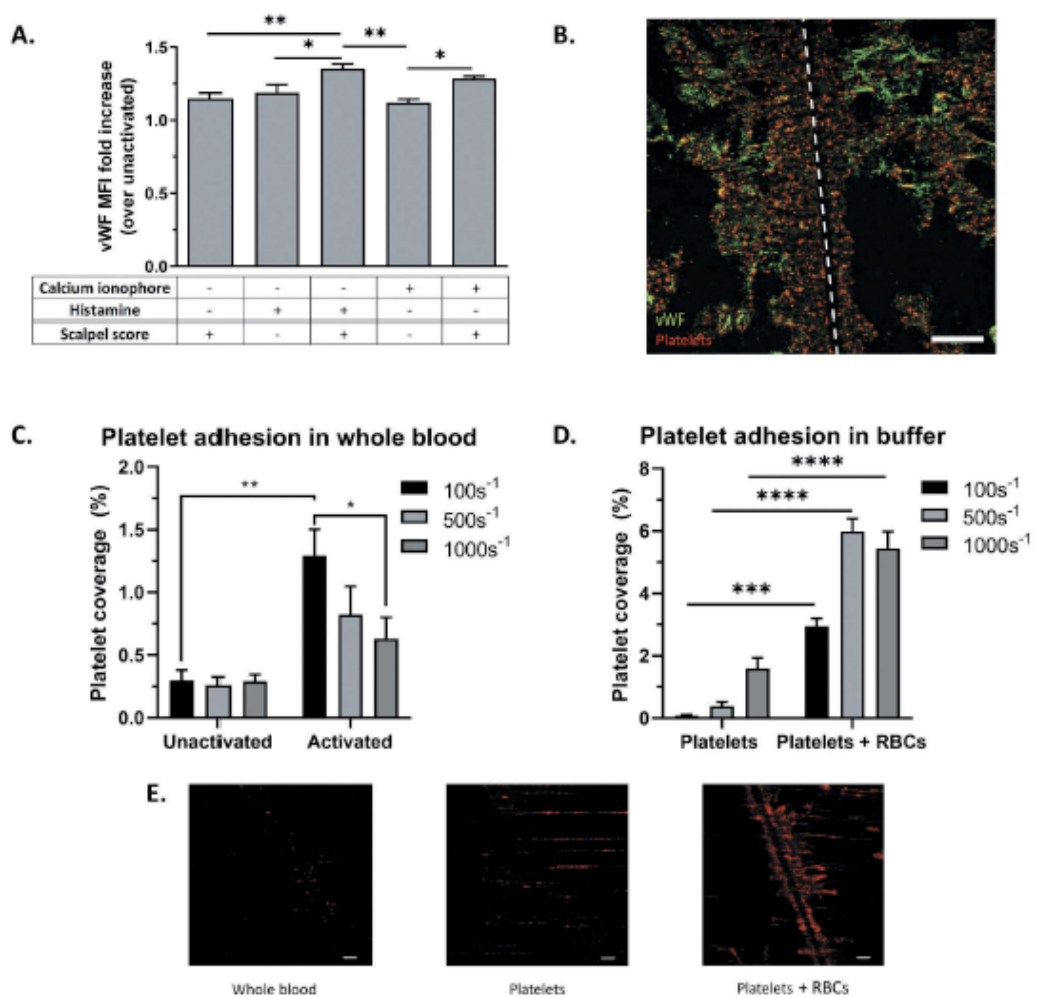
607

608

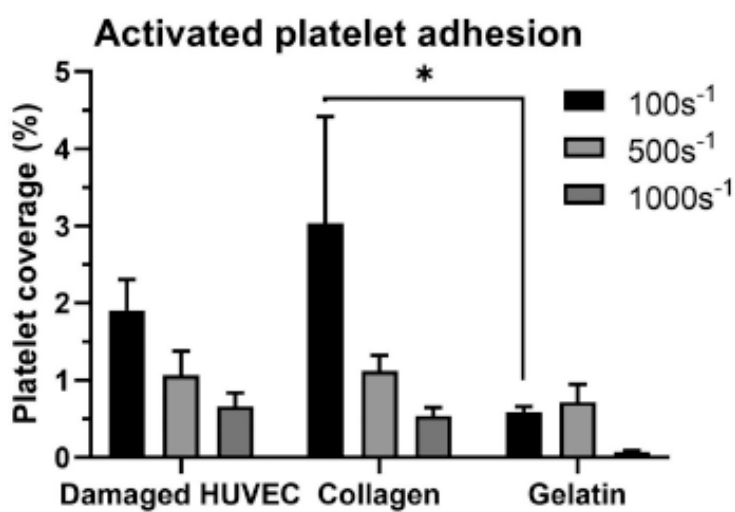
609

610 FIGURES

611 Figure 1

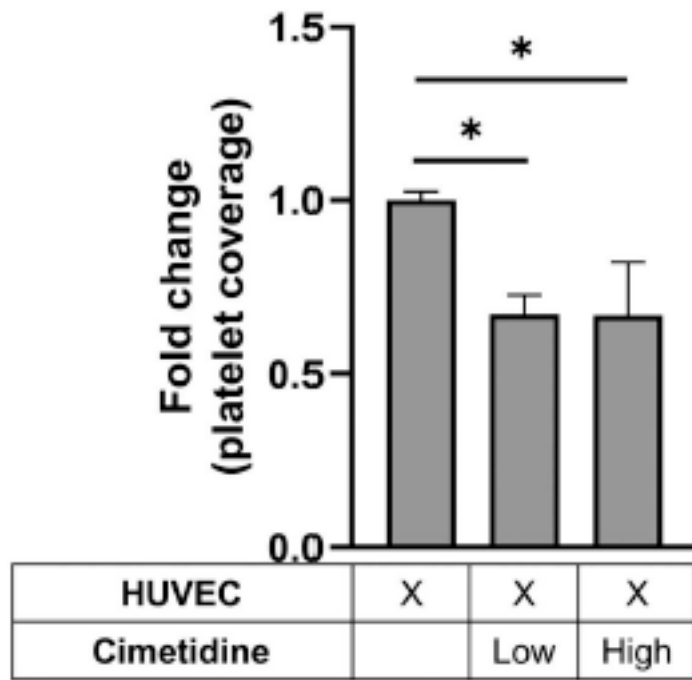
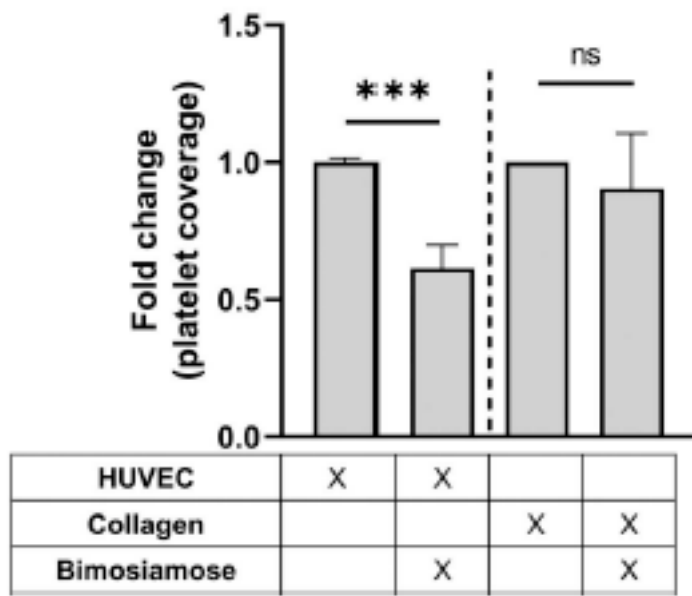


613 Figure 2



614

615 Figure 3



Supplemental File

An *in vitro* blood flow model to advance the study of platelet adhesion utilizing a damaged endothelium

Alison Leigh Banka^a, and Omolola Eniola-Adefeso^{a,b*}

^a*Department of Chemical Engineering, University of Michigan, Ann Arbor, United States of America;* ^b*Department of Biomedical Engineering, University of Michigan, Ann Arbor, United States of America*

*Corresponding author. Email: lolaa@umich.edu

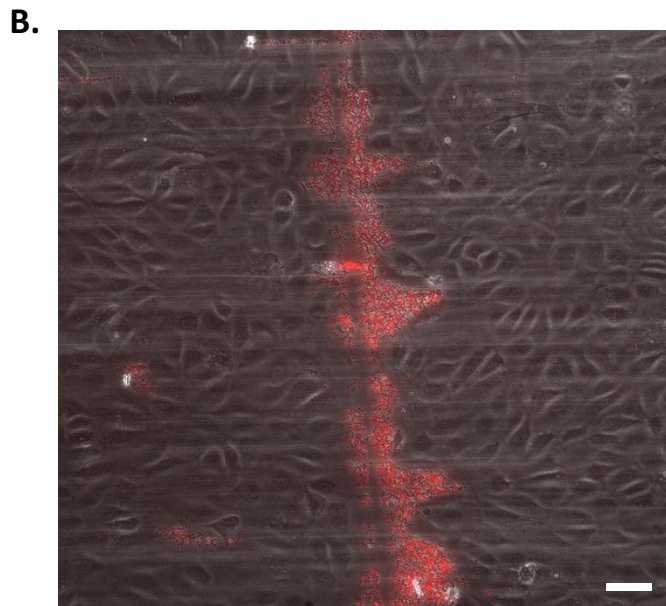
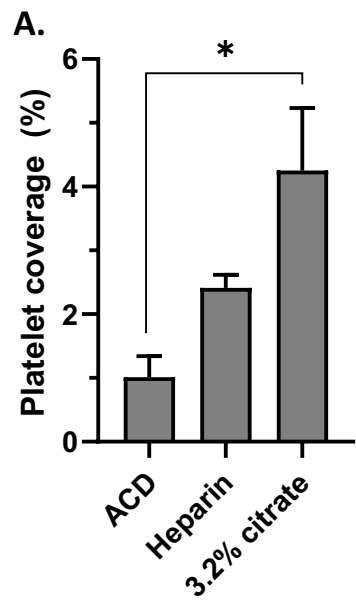


Fig. S1: Platelet adhesion on ‘damaged’ HUVEC with different anticoagulants. (A) Platelet adhesion (% of total surface area) of activated platelets after 5 minutes of laminar flow in whole blood at 40% hematocrit and 1000s^{-1} using different anticoagulants, (B) Platelet adhesion in heparinized blood of activated, anti-CD41/61 PE-stained platelets (red) overlaid on top of a HUVEC monolayer activated with histamine and manually damaged with scalpel. Scale bar, 100 μm . Statistical analysis was performed using one-way ANOVA with Tukey’s multiple comparisons test, where (*) indicates $p<0.05$.

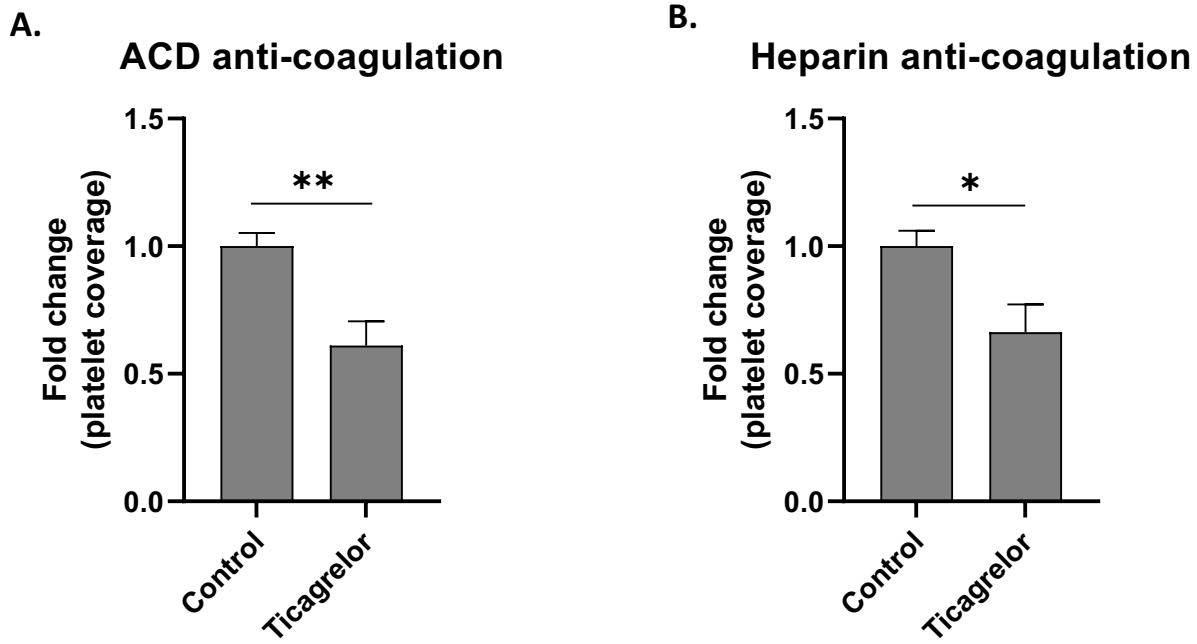


Fig. S2: Impact of Ticagrelor on platelet adhesion. Platelet adhesion (% of total surface area) of activated platelets after 1 hour treatment with 10 μ M ticagrelor using (A) ACD or, (B) heparin-anticoagulated whole blood. Blood was perfused for 5 minutes of laminar flow at 40% hematocrit and 1000s^{-1} over an activated, damaged HUVEC monolayer. Statistical analysis was performed using an unpaired t-test, where (*) indicates $p<0.05$ and (**) indicates $p<0.01$.

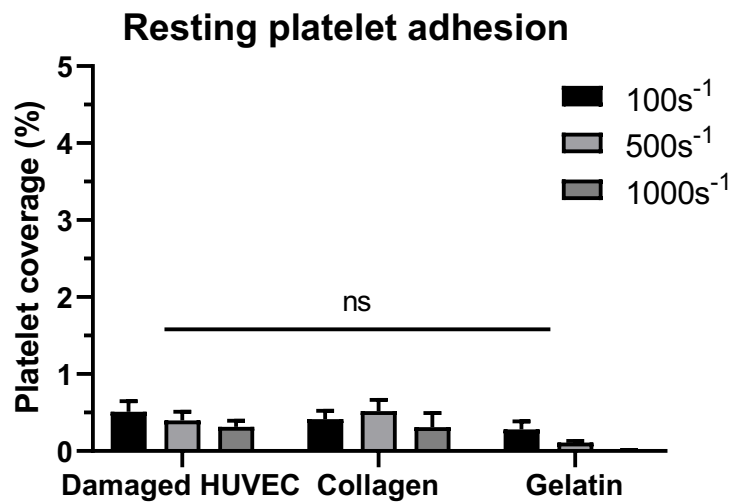


Fig. S3: Resting platelet adhesion on damaged endothelium compared to control utilizing collagen and gelatin. Platelet coverage (as % of total surface area of photo) on damaged endothelium, collagen (1 mg/mL), or gelatin (1 mg/mL) of resting platelets in whole blood at 40% hematocrit after 5 minutes of laminar flow. Statistical analyses were performed using two-way ANOVA with Tukey's multiple comparisons test.

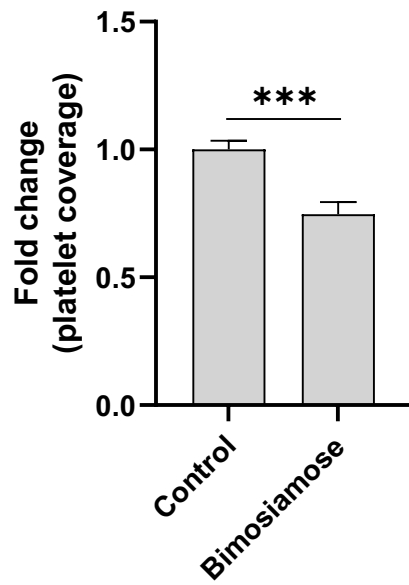


Fig. S4: Impact of Bimosiamose on heparinized platelet adhesion. Platelet adhesion (% of total surface area) of activated platelets after 1 hour treatment with 50 μ M Bimosiamose using heparin-anticoagulated whole blood. Blood was perfused for 5 minutes of laminar flow at 40% hematocrit and 1000s^{-1} over an activated, damaged HUVEC monolayer. Statistical analysis was performed using an unpaired t-test, where (***) indicates $p<0.001$.